DOI: 10.1002/cssc.201200655

Co-sensitization of Organic Dyes for Efficient Dye-Sensitized Solar Cells

Ming Cheng,[a] Xichuan Yang,*[a] Jiajia Li,[a] Fuguo Zhang,[a] and Licheng Sun*[a, b]

Novel cyanine dyes, in which a tetrahydroquinoline derivative is used as an electron donor and 1-butyl-5-carboxy-3, 3-dimethyl-indol-1-ium moiety is used as an electron acceptor and anchoring group, were designed and synthesized for application in dye-sensitized solar cells. The photovoltaic performance of these solar cells depends markedly on the molecular structure of the dyes in terms of the *n*-hexyl chains and the methoxyl unit. Retardation of charge recombination caused by the introduction of *n*-hexyl chains resulted in an increase in electron lifetime. As a consequence, an improvement of open-circuit photovoltage (V_{oc}) was achieved. Also, the electron injection efficiencies were improved by the introduction of methoxyl moiety, which led to a higher short-circuit photocurrent density (J_{sc}). The highest average efficiency of the sensitized devices (η) was 5.6% ($J_{sc}=13.3$ mA cm^{-2}, $V_{oc}=606$ mV, and fill factor $FF=69.1$%) under 100 mW cm^{-2} (AM 1.5G) solar irradiation. All of these dyes have very high absorption extinction coefficients and strong absorption in a relatively narrow spectrum range (500–650 nm), so one of our organic dyes was explored as a sensitizer in co-sensitized solar cells in combination with the other two other existing organic dyes. Interestingly, a considerably improved photovoltaic performance of 8.2% ($J_{sc}=20.1$ mA cm^{-2}, $V_{oc}=597$ mV, and $FF=68.3$%) was achieved and the device showed a panchromatic response with a high incident photon-to-current conversion efficiency exceeding 85% in the range of 400–700 nm.

Introduction

Dye-sensitized solar cells (DSSCs) are regarded as a low-cost next-generation solar cells, and significant progress has been made since their inception in 1991.[1] However, it is necessary to further improve the energy conversion efficiency of DSSCs to enable successful commercialization. To achieve this goal, the photosensitizer needs to capture as much incident light as possible, both in the absorption intensity and the absorption breadth. Many attempts, such as tandem DSSCs and co-sensitized DSSCs, have been conducted to broaden the absorption spectra of the cells.[2–17] For example, the co-sensitization of a porphyrin dye YD2-o-C8 and a metal-free dye Y123 with complementary spectral responses showed an efficiency of 12.3%, a considerably higher photovoltaic performance than the devices fabricated with the individual dye.[6] A phthalocyanine dye (TT1 or PcS15) co-sensitized with various organic dyes (JK2, D2, or D131) exhibited an enhanced device performance through the improved light-harvesting efficiency of the cell.[9,10,16] The co-sensitization of TiO_2 films by a black dye and organic dyes (D131 or Y1) resulted in a significantly enhanced photocurrent, leading to a device performance of 11.0–11.4%.[11,12] These works have shown a clear advance towards efficient DSSCs based on the system with an extended spectrum response in the red to near-IR region. Cyanine dyes have very high absorption extinction coefficients (about 10^5 M^{-1} cm^{-1}), an intense but narrow absorption band in the long wavelength region. This makes them good candidates for co-sensitizers owing to the less competitive absorption with dyes absorbing in the short wavelength region and the near infrared (NIR) region. We have designed and synthesized four cyanine dyes CM201–CM204 (see Figure 1), in which a tetrahydroquinoline derivative is used as an electron donor and 1-butyl-5-carboxy-3, 3-dimethyl-indol-1-ium moiety is used as an electron acceptor and anchoring group, and applied these dyes to DSSCs. The dye CM203 was also applied to co-sensitize with the other two organic dyes CMR103 and HY113 (see Figure 7).

[a] Dr. M. Cheng, Prof. X. Yang, Dr. J. Li, Dr. F. Zhang, Prof. L. Sun
State Key Laboratory of Fine Chemicals
DUT-KTH Joint Education and Research Centre on Molecular Devices
Dalian University of Technology (DUT)
2 Linggong Rd., 116024 Dalian (P.R. China)
Fax: (+86) 411-84986250
E-mail: yangxc@dlut.edu.cn

[b] Prof. L. Sun
School of Chemical Science and Engineering
Center of Molecular Devices, Department of Chemistry
Royal Institute of Technology (KTH)
Teknikringen 42, SE 100 44 Stockholm (Sweden)

Supporting Information for this article is available on the WWW under http://dx.doi.org/10.1002/cssc.201200655.

Results and Discussion

Photophysical and electrochemical properties of CM201–CM204

The absorption spectra recorded for the dyes in dichloromethane solution are displayed in Figure 2. All of the dyes exhibit a prominent peak around 578–604 nm (Table 1 and Figure 2) with a molar extinction coefficient from 3.9×10^4 to 4.0×10^4 M^{-1} cm^{-1}. Figure 3 shows the absorption spectra of four

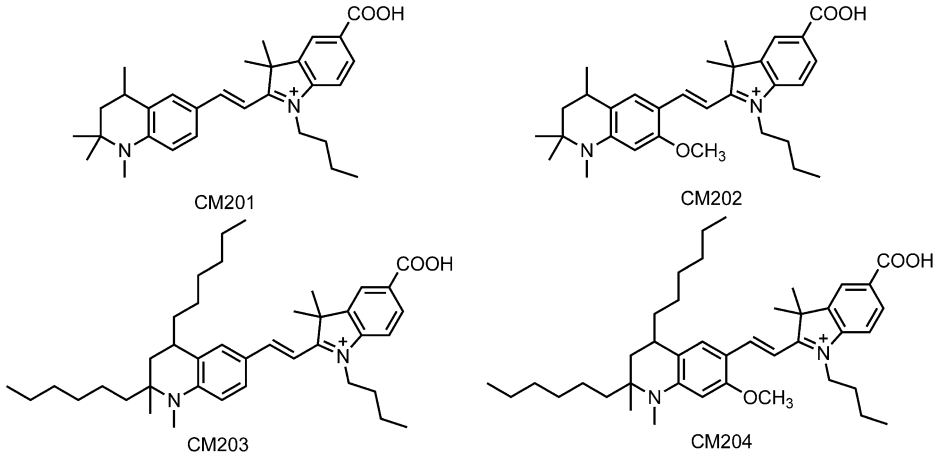

Figure 1. Structure of the cyanine dyes CM201–CM204.

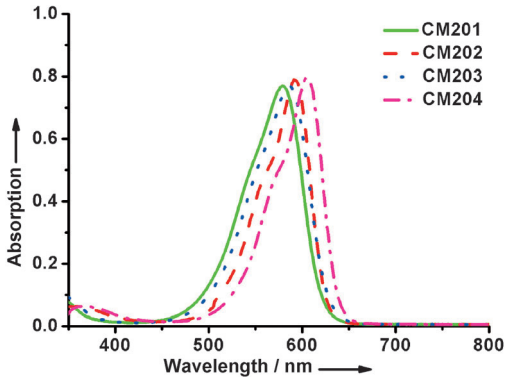

Figure 2. Absorption spectra of CM201–CM204 in CH_2Cl_2 (2.0×10^{-5} M).

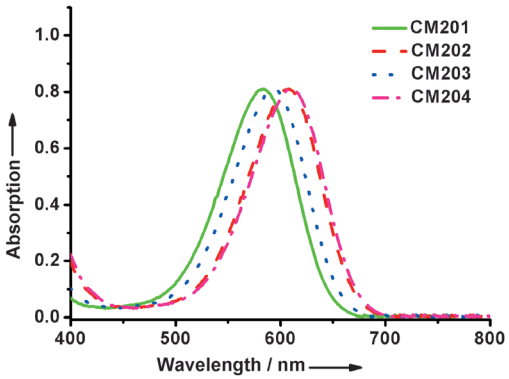

Figure 3. Absorption spectra of CM201–CM204 on TiO_2 films.

Table 1. UV/Vis absorption and electrochemical properties of the dyes CM201–CM204.

Dye	λ_{max}[a] in CH_2Cl_2 [nm]	ε at λ_{max} [$M^{-1}cm^{-1}$]	λ_{max}[b] on TiO_2 [nm]	$E_{0\text{-}0}$ [V][c]	E_{ox}[d] [V]	E_{LUMO}[e] [V]
CM201	578	38600	583	1.79	0.96	−0.83
CM202	593	40100	607	1.74	0.80	−0.94
CM203	586	38500	593	1.73	0.84	−0.89
CM204	604	40300	610	1.69	0.74	−0.95

[a] Absorption spectra in solution were measured in CH_2Cl_2 (2×10^{-5} M). [b] Absorption spectra on TiO_2 film were measured with dye-loaded TiO_2 films immerged in CH_2Cl_2 solution. [c] The energy gap $E_{0\text{-}0}$ was determined from the intersection of the tangent of absorption on TiO_2 film and the X axis at $1240/\lambda$. [d] The oxidation potentials of the dyes were measured in CH_2Cl_2 solutions with tetrabutylammonium hexafluorophosphate ($TBAPF_6$, 0.1 M) as electrolyte, ferrocene/ferrocenium (Fc/Fc^+) as an internal reference and converted to NHE by adding 440 mV. [e] E_{LUMO} (versus NHE) was calculated according to $E_{LUMO}=E_{ox}-E_{0\text{-}0}$.

dyes adsorbed on the surfaces of the TiO_2 films. It can be seen that upon anchoring the dyes to the TiO_2 surface, the absorption spectra red shifted around 5–14 nm and became broader than those in solution.

The cyclic voltammograms (CV) of the four dyes show quasi-reversible couples. The HOMO levels of CM201, CM202, CM203, and CM204 corresponding to their first redox potentials are 0.96, 0.80, 0.84, and 0.74 V versus standard hydrogen electrode (NHE), respectively. These values are more positive than the potential of S^{2-}/S_x^{2-} couple (+0.5 V versus NHE),[18] indicating the oxidized dyes can be regenerated thermodynamically.[19–21] The estimated excited-state potential corresponding to the LUMO levels of the dyes CM201–CM204 are −0.83 V, −0.93 V, −0.89 V, and −0.95 V versus NHE, respectively, which are more negative than the conduction band edge of TiO_2 (about −0.5 V versus NHE).[19] Therefore, the energy surplus of the LUMO in four dyes allows the injection of electrons into the conduction band of TiO_2.

Photocurrent–voltage characteristics of devices sensitized by CM201–CM204

The dye-sensitized solar cells using these dyes as sensitizers for nano-crystalline anatase TiO_2 were fabricated, and the device performance parameters under AM 1.5G illumination are shown in Table 2. Figure 4 and Figure 5 show the photocur-

Table 2. Photovoltaic performances[a] of the DSSCs sensitized by CM201–CM204.

Dye[b]	J_{sc} [mA cm^{-2}]	V_{oc} [mV]	*FF* [%]	η [%]
CM201	11.7±0.2	580±5	70.1±1.2	4.7±0.1
CM202	12.4±0.1	588±4	68.7±1.0	5.0±0.2
CM203	12.2±0.1	596±3	68.9±0.5	5.0±0.1
CM204	13.3±0.2	606±4	69.1±0.8	5.5±0.1

[a] Performances of DSSCs were measured by using a 0.159 cm^2 working area under 100 mW cm^{-2}. [b] The concentration of the dye bath is 2×10^{-4} M in CH_2Cl_2. Electrolyte: 0.6 M 1,2-dimethyl-3-propylimidazolium iodide (DMPII), 0.3 M LiI, 0.02 M S_x^{2-}, 0.02 M S in acetonitrile (AN).

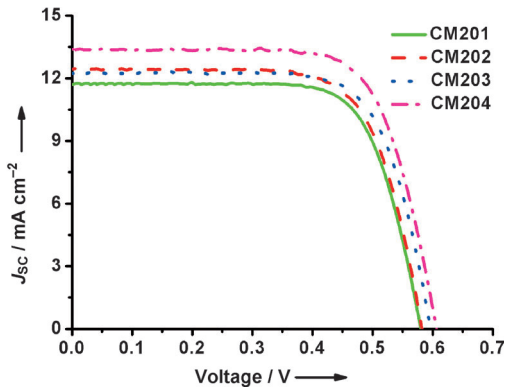

Figure 4. *J–V* curves of DSSCs sensitized by CM201–CM204.

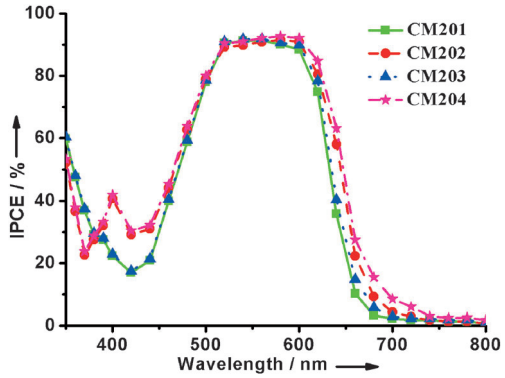

Figure 5. IPCE spectra of DSSCs sensitized by CM201–CM204.

rent-voltage (*J–V*) curves and the incident photon-to-current conversion efficiencies (IPCE). Under standard global AM 1.5G solar conditions, the devices using dye CM204 exhibited the best efficiency giving a short-circuit photocurrent density (J_{sc}) of 13.3 mA cm^{-2}, an open- circuit voltage (V_{oc}) of 606 mV, and a fill factor (*FF*) of 69.1%, corresponding to an overall conversion efficiency (η) of 5.5%. According to the IPCE spectra, the integral current density is 13.7 mA cm^{-2}, which considering the error is in good agreement with the measured photocurrent density. The devices sensitized by the dyes CM201, CM202, and CM203 showed efficiencies in the range of 4.7–5.0% (see Table 2). Kroeze et al.[22] reported that, in the presence of alkyl substitution in the dye structure, V_{oc} can be improved owing to the inhibition of charge recombination resulting from the blocking effect of the substituent on the TiO_2 surface. Therefore, we introduced the *n*-hexyl chains into the dyes CM203 and CM204. From the test results (Table 2), we indeed observed that the V_{oc} of the device sensitized by CM203 is higher (16 mV) than that of the device sensitized by CM201, yielding a higher efficiency for CM203. A similar result was found in the devices sensitized by CM202 and CM204. The V_{oc} of the device sensitized by CM204 was 18 mV higher than that of the device sensitized by CM202. These results indicate that the charge recombination was effectively suppressed by the blocking effect of the long alkyl chain.(CDCA was added in every case, so the V_{oc} difference between CM201 and CM203, or CM202 and CM204, was just caused by the alkyl chain and was not related to CDCA).

Electrochemical impedance spectroscopy analysis of devices sensitized by CM201–CM204

Electrochemical Impedance Spectroscopy (EIS) analysis was used to study the interfacial charge transfer processes in DSSCs. The measurements were scanned from 10^6 to 10^{-2} Hz at room temperature in dark condition with an applied bias voltage of −0.70 V. Nyquist plots and Bode phase plots for the devices sensitized by CM201–CM204 are shown in Figure 6.

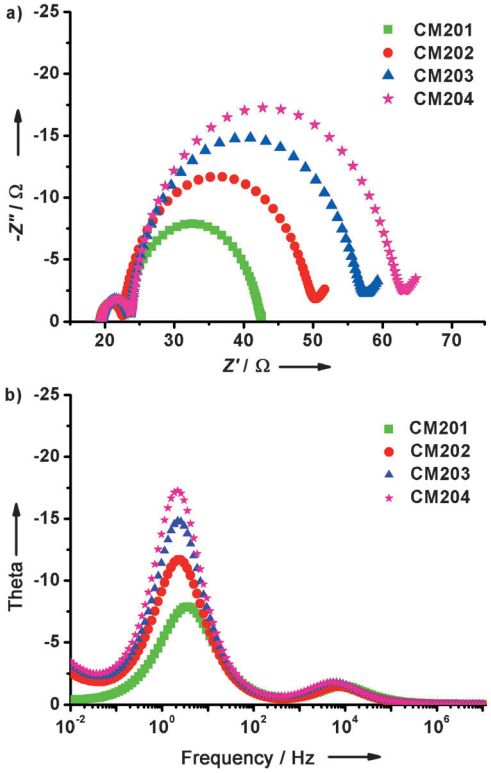

Figure 6. a) Nyquist plots and b) Bode phase plots of DSSCs sensitized by CM201–CM204.

Some important parameters can be obtained by fitting the EIS spectra to an electrochemical model.[23] R_S, R_{rec}, and R_{CE} represent the series resistance and the charge-transfer resistances at the dye/TiO_2/electrolyte interface (recombination resistance) and the counter electrode (CE), respectively. From the EIS measurements, the electron lifetime (τ_e) expressing the electron recombination between the electrolyte and TiO_2 may be extracted from the angular frequency (ω_{rec}) at the mid frequency peak in the Bode phase plots using the relation $\tau_e = 1/\omega_{rec}$. The diameters of the medium-frequency semicircle, corresponding to R_{rec}, decrease in the order CM204 (37.8 Ω) > CM203 (32.6 Ω) > CM202 (26.7 Ω) > CM201 (20.1 Ω), implying that the recombination reaction between the conduction band electrons in TiO_2 film and electrolyte is better inhibited for CM203 and CM204 than for CM201 and CM202 because of the

introduction of *n*-hexyl. As a consequence, an improvement in V_{oc} was achieved. The electron recombination lifetimes (τ) calculated from the angular frequency (ω_{min}) at the intermediate-frequency peak in the Bode phase plots (Figure 6b) using $\tau = 1/\omega_{min}$ also indicated the trend (see Figure 6b and Table 3).

Table 3. Parameters obtained by fitting the EIS spectra to an electrochemical model.

Dye	R_s [Ω]	R_{rec} [Ω]	R_{ce} [Ω]	Lifetimes [s]
CM201	19.4	20.1	3.2	0.28
CM202	19.3	26.7	3.2	0.45
CM203	19.5	32.6	4.0	0.46
CM204	19.5	37.8	4.2	0.47

Photophysical, photocurrent–voltage characteristics of co-sensitized DSSCs

As mentioned above, in spite of the high ε of organic dyes CM201–CM204, the narrow spectrum response (500–650 nm) limits the light absorption to the visible region leading to lower DSSC efficiencies compared to the ruthenium complex N719. So the other two metal-free organic dyes CMR103 and HY113 reported by our group earlier[24,25] were selected as co-sensitizers with CM203 to enhance the light harvesting efficiency in DSSC applications. The structures of CMR103 and HY113 are shown in Figure 7. The absorption spectrum of CMR103, CM203, HY113, and the co-absorption of the three dyes on TiO_2 films are shown in Figure 8. Dye CMR103 has a strong absorption in the range of 400–500 nm, and HY113 shows intense absorption in the NIR region (600–700 nm). The co-sensitized TiO_2 film exhibits three absorption peaks and broad absorption in 400–700 nm regions.

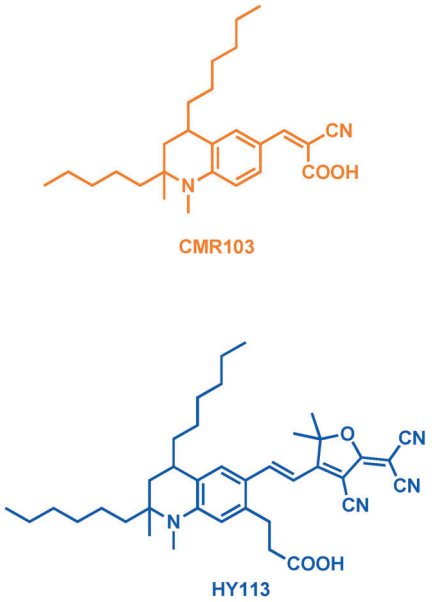

Figure 7. Structures of the dyes CMR103 and HY113.

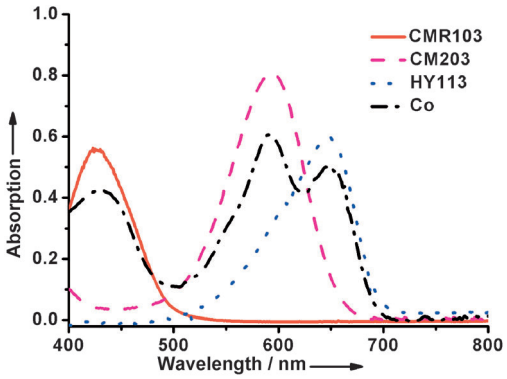

Figure 8. Absorption spectra of CMR103, CM203, HY113, and co-adsorption on TiO_2 films.

The *J*–*V* curves of solar cells with CMR103, CM203, HY113, and the co-sensitization of three dyes are shown in Figure 9. The corresponding photovoltaic parameters of these solar cells

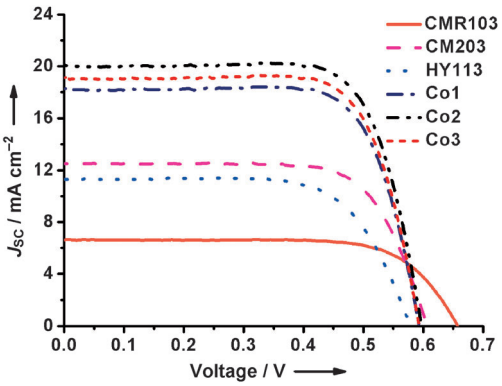

Figure 9. *J*–*V* curves and photos of DSSCs sensitized by CMR103, CM203, HY113, and co-sensitization.

are presented in Table 4. The power conversion efficiencies (at AM 1.5G illumination) of devices based on individual CMR103, CM203, and HY113 were 3.1, 5.0, and 4.4%, respectively. Importantly, the co-sensitized solar cell showed much higher photo-

Table 4. Photovoltaic performances[a] of DSSCs sensitized by TQ1, M203, HY113, and co-sensitization.

Dye[b]	J_{sc} [mA cm^{-2}]	V_{oc} [mV]	*FF* [%]	η [%]
CMR103	6.6±0.2	660±3	71.1±1.0	3.1±0.2
CM203	12.2±0.1	596±4	68.9±0.6	5.0±0.2
HY113	11.3±0.1	570±5	69.3±0.5	4.4±0.2
Co1	18.3±0.3	595±5	69.1±0.5	7.5±0.2
Co2	20.1±0.2	597±5	68.3±1.0	8.2±0.2
Co3	19.1±0.2	595±4	68.7±0.6	7.8±0.2

[a] Performances of the DSSCs were measured by using a 0.159 cm^2 working area under 100 mW cm^{-2} (AM 1.5G) condition. Electrolyte: 0.6 M DMPII, 0.3 M LiI,0.02 M S_x^{2-},0.02 M S. [b] The concentration of the dye bath is 2×10^{-4} M in CH_2Cl_2.

current and efficiency than those of the individual dye-sensitized cells. The absorption and desorption of the sensitizer is a balance during the sensitization. To obtain a high J_{sc}, it is necessary to make full use of the NIR region. In our experiment, we found that the dye HY113 is easily desorbed during the sensitization of other dyes. Correspondingly, the photocurrent depends on the soaking sequence of the three dyes CMR103, CM203, and HY113. For the co-sensitized device Co2, a TiO_2 film was firstly dipped in the CMR103 dye solution (0.5 h), then dipped in the CM203 dye solution (0.5 h), followed by dipping in the HY113 dye solution (4 h). The resulting photovoltaic parameters J_{sc}, V_{oc}, FF, and η were 597 mV, 20.1 mA cm^{-2}, 68.3 %, and 8.2 %, respectively. According to the IPCE spectra, the integral current density was 19.8 mA cm^{-2} (see Figure 10), which considering the error matches well with the measured photocurrent density. These results show a superior photovoltaic performance for the co-sensitization of three organic dyes compared to that of the individual dye-sensitized solar cells.

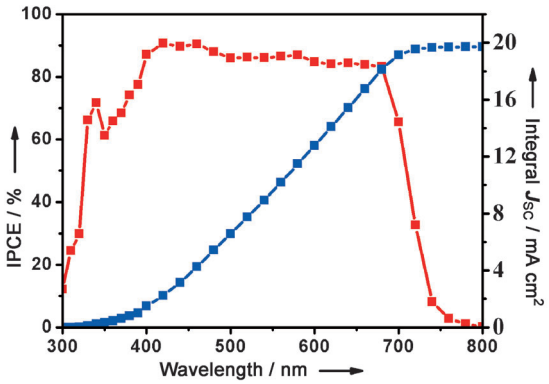

Figure 10. IPCE and integral current density of the co-sensitized device Co2.

The IPCE spectra of devices sensitized by CMR103, CM203, HY113, and co-sensitization were plotted as a function of excitation wavelength and are presented in Figure 10. From the experiments, it was found that the IPCE of the co-sensitized devices depended greatly on the dipping sequence and time of the electrode in different dye solutions. The largest increase in the IPCE region was observed in the region in which the final dye was deposited. The co-sensitized device Co1 was fabricated by the following steps: co-sensitization of TiO_2 films was first done by dipping the in the HY113 dye solution (4 h), then by dipping in the CM203 dye solution (1 h), followed by dipping in the CMR103 dye solution (1 h). The co-sensitized device Co3 was sensitized in the following sequence: co-sensitization of TiO_2 films was first achieved by dipping in the CM203 dye solution (1 h), then by dipping in the CMR103 dye solution (1 h), followed by dipping in the HY113 dye solution (4 h). For the Co1 device, the IPCE value in the NIR region was much lower but much higher in 400–550 nm region than the other devices. The HY113 sensitized Co2 device showed the highest IPCE value in the NIR region and the highest J_{sc}. The IPCE spectrum shows that solar cells sensitized by individual

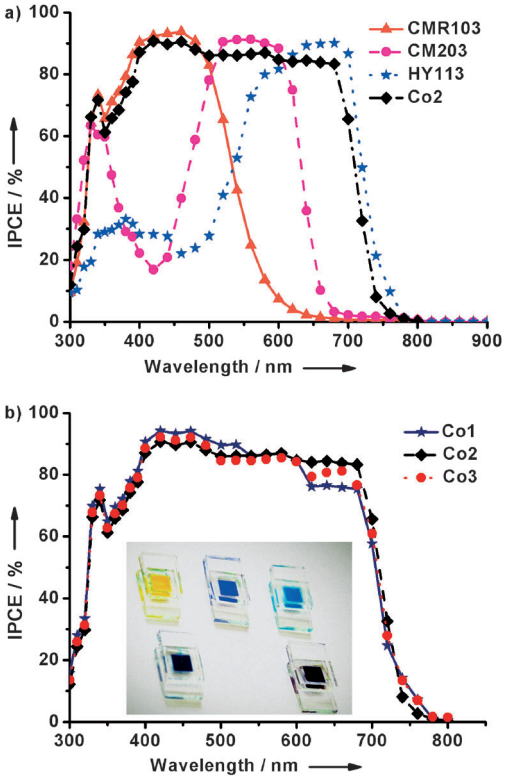

Figure 11. IPCE spectra of DSSCs sensitized by CMR103, CM203, HY113, and co-sensitization (photo of DSSCs inserted). The devices Co1, Co2, and Co3 were sensitized with different soaking sequences of the three dyes CMR103, CM203, and HY113.

CMR103, CM203, and HY113 dyes have peak efficiencies of 94 (460 nm), 91 (560 nm), and 90 % (660–680 nm), respectively. The IPCE spectrum of the solar cell based on co-sensitization by CMR103, CM203, and HY113 dyes exhibits an impressive panchromatic response from 400 to 700 nm. This shows that the three organic dyes were efficiently co-adsorbed on the surface of TiO_2. Co-sensitization of the TiO_2 electrodes markedly increased the current density as reported in Table 4 and extended the spectral response to the whole visible domain and consequently enhanced the photocurrent performance.

Electrochemical impedance spectroscopy analysis of co-sensitized DSSCs

From the EIS spectra of DSSCs sensitized by CMR103, CM203, HY113, and co-sensitization (see Figure 12), we can see that the diameters of the medium frequency semicircle, corresponding to R_{rec}, vary considerably. The R_{rec} values are 39.1, 32.6, and 21.1 Ω for DSSCs sensitized by CMR103, CM203, and HY113, respectively. For the co-sensitized device Co2, R_{rec} was 32.7 Ω. The R_{rec} of DSSCs decrease in the order of CMR103 > Co2 > CM203 > HY113, corresponding to the decrease of voltage. The recombination reaction between the conduction-band electron in TiO_2 films and electrolyte is better inhibited for the co-sensitized solar cells compared with the device sensitized by CM203 and HY113. The Bode phase plots showed the same trends.

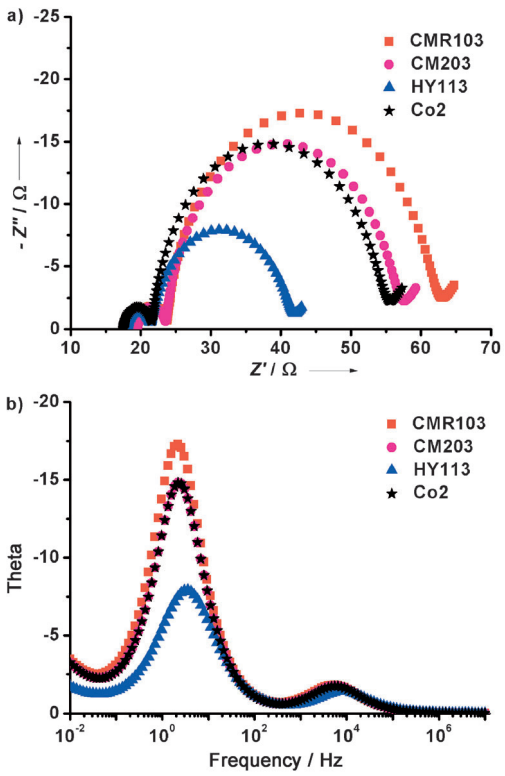

Figure 12. a) Nyquist plots and b) Bode phase plots of DSSCs sensitized by CMR103, CM203, HY113, and co-sensitized device Co2.

Experimental Section

The dyes were synthesized by the stepwise synthetic protocol shown in Schemes 1–3 according to previous literature.[24–29] ^{1}H NMR spectra were recorded (VARIAN INOVA 400 MHz spectrometer, USA) using tetramethylsilane as standard. MS data were obtained by using GCT CA156 (UK), HP1100 LC/MSD (USA), and LC/Q-TOF MS (UK). Absorption spectra were recorded on a HP8453 (USA). Electrochemical redox potentials were obtained by means of cyclic voltammetry (CV) on an electrochemistry workstation (BAS100B, USA). The working electrode was a glass carbon disk, the auxiliary electrode was a Pt wire, and Ag/Ag^+ was used as the reference electrode. $TBAPF_6$ was used as a supporting electrolyte in AN. The Fc/Fc^+ redox couple was used as an internal reference. The potentials versus NHE were calibrated by adding 440 mV to the potentials versus Fc/Fc^+. EIS was measured with an impedance/gain-phase analyzer (PARSTAT 2273, USA) under dark conditions, with a forward bias of −0.7 V.

The DSSCs sensitized by dyes CM201–CM204 were fabricated according to previous literature with modifications.[24] A layer of 2 μm TiO_2 (13 nm paste, Heptachroma, China) was coated on F-doped tin oxide conducting glass (TEC15, 15 Ω/square, Pilkington, USA) by screen printing and then dried for 5 min at 125 °C. This procedure was repeated six times (12 μm) and finally the electrode was coated with a layer (4 μm) of TiO_2 paste (DHS-SLP1, Heptachroma, China) as the scattering layer. The double-layer TiO_2 electrodes (area: 6×6 mm) were heated under an air flow (520 °, 30 min) and then cooled to room temperature. The sintered film was further treated with $TiCl_4$ aqueous solution (40 mM, 70 °C, 30 min), then washed with water, and annealed (520 °C, 30 min). After the film was cooled to room temperature, it was immersed into a dye bath

Conclusions

We designed, synthesized, and systematically investigated four cyanine dyes CM201–CM204. Among the four cyanine dyes, the devices sensitized by CM204 generated the highest efficiencies of 5.5%, with a short-circuit photocurrent density of 13.3 mA cm^{-2}, an open-circuit voltage of 606 mV, and a fill factor of 69.1%. All of the four dyes CM201–CM204 had very high absorption extinction coefficients and a strong absorption within a relatively narrow spectrum range (500–650 nm). Upon exploration of CM203 as co-sensitizer in combination with two other organic dyes, CMR103 and HY113, a considerably improved efficiency of 8.2% was achieved (J_{sc} = 20.1 mA cm^{-2}, V_{oc} = 597 mV, and FF = 68.3%). This is much higher than that of an individual dye-sensitized solar cell. More importantly, the co-sensitized devices having complementary spectral responses provided a remarkable increase in the photocurrent and hence enhanced the power conversion efficiency. The IPCE spectra of cells based on co-sensitization showed a panchromatic response with >80% efficiency over the entire visible spectral region (400–700 nm). Using this strategy, we can conveniently utilize a wide region of the solar spectrum by co-sensitizing dyes that have complementary spectral responses.

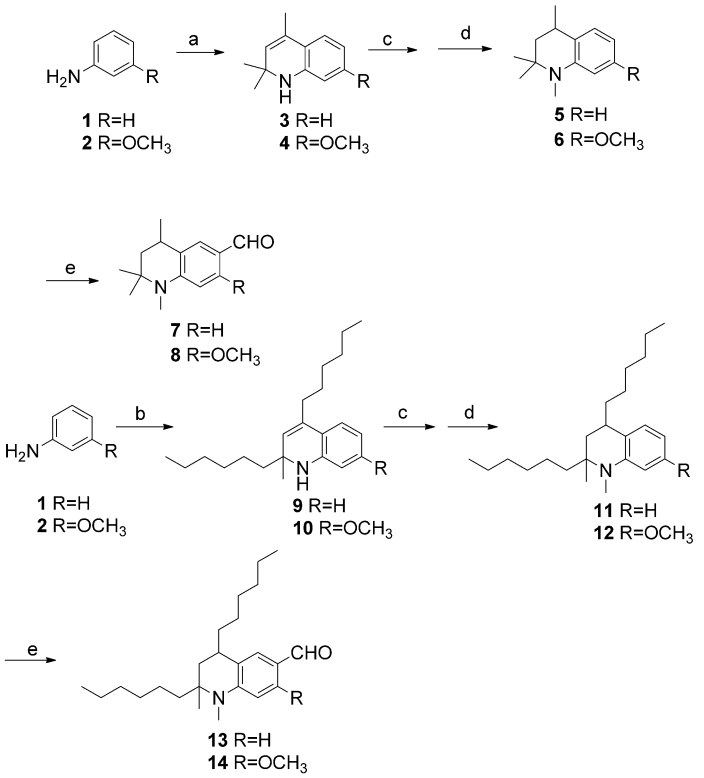

Scheme 1. Synthetic routes for the electron donor: a) acetone, *p*-TsOH, cyclohexane, 80–90 °C, 8–10 h; b) 2-octanone, *p*-TsOH, toluene, 125 °C, 8–10 h; c) Raney-Ni, H_2, 1 MPa, 120 °C; d) $(CH_3)_2SO_4$, benzene, 85 °C, 24 h; e) dimethylformamide/$POCl_3$, 55 °C, 6 h.

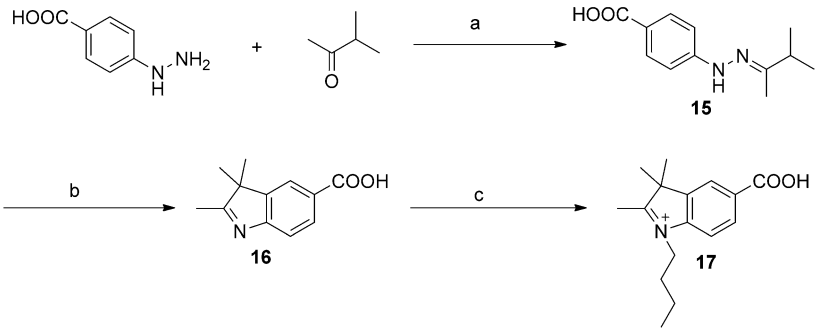

Scheme 2. Synthetic routes for the electron acceptor: a) EtOH, reflux 4 h, b) AcOH, reflux 4 h, c) *n*-C_4H_9I, CH_3CN, 85 °C, 24 h.

(2×10^{-4} M). The electrode was then rinsed with EtOH and dried. The hermetically sealed cells were fabricated by assembling the dye-loaded film as the working electrode and Pt-coated conducting glass as the counter electrode separated with a hot-melt Surlyn 1702 film (25 μm, Dupont). Light source for *J–V* measurement was an AM 1.5G solar simulator (16S-002, Solar Light Co. Ltd., USA). The incident light intensity (100 mW cm^{-2}) was calibrated with a standard Si solar cell. The solar cells tested were masked to a working area of 0.159 cm^2. The *J–V* curves were obtained by the LSV method using an electrochemical workstation (LK9805, Lanlike Co. Ltd., China). The measurement of IPCE was performed a Hypermono-light (SM-25, Jasco Co. Ltd., Japan). The J_{sc} was calibrated by integrating the IPCE value tuned light density of AM 1.5G against wavelength.

Acknowledgements

We gratefully acknowledge the financial support of this work from China Natural Science Foundation (Grant 21076039, Grant 20120102036), the National Basic Research Program of China (Grant No. 2009CB220009), the Ministry of Science and Technology (MOST) (Grant 2001CCA02500), the Swedish Energy Agency, K&A Wallenberg Foundation, the State Key Laboratory of Fine Chemicals (KF0805), and the Program for Innovative Research Team of Liaoning Province (Grant No. LS2010042).

Keywords: cyanines · dyes/pigments · sensitizers · solar cells

[1] B. O'Regan, M. Grätzel, *Nature* **1991**, *353*, 737–740.
[2] L. Li, Y. Hao, X. Yang, J. Zhao, H. Tian, C. Teng, A. Hagfeldt, L. Sun, *ChemSusChem* **2011**, *4*, 609–612.
[3] J. N. Clifford, E. Palomares, M. K. Nazeeruddin, R. Thampi, M. Grätzel, J. R. Durrant, *J. Am. Chem. Soc.* **2004**, *126*, 5670–5671.
[4] H. Choi, S. Kim, S. O. Kang, J. Ko, M. S. Kang, J. N. Clifford, A. Forneli, E. Palomares, M. K. Nazeeruddin, M. Grätzel, *Angew. Chem.* **2008**, *120*, 8383–8387; *Angew. Chem. Int. Ed.* **2008**, *47*, 8259–8263.
[5] K. Lee, S. W. Park, M. J. Ko, K. Kim, N. G. Park, *Nat. Mater.* **2009**, *8*, 665–671.
[6] A. Yella, H.-W. Lee, H. N. Tsao, C. Yi, A. K. Chandiran, M. K. Nazeeruddin, E. W.-G. Diau, C.-Y. Yeh, S. M. Zakeeruddin, M. Grätzel, *Science* **2011**, *334*, 629–634.
[7] M. Murayama, T. Mori, *Thin Solid Films* **2008**, *516*, 2716–2722.
[8] D. Kuang, P. Walter, F. Nüesch, S. Kim, J. J. Ko, P. Comte, S. M. Zakeeruddin, M. K. Nazeeruddin, M. Grätzel, *Langmuir* **2007**, *23*, 10906–10909.
[9] J.-J. Cid, J.-H. Yum, S.-R. Jang, M. K. Nazeeruddin, E. Martinez-Ferrero, E. Palomares, J. J. Ko, M. Grätzel, T. Torres, *Angew. Chem.* **2007**, *119*, 8510–8514; *Angew. Chem. Int. Ed.* **2007**, *46*, 8358–8362.
[10] J. N. Clifford, A. Forneli, H. Chen, T. Torres, S. Tan, E. Palomares, *J. Mater. Chem.* **2011**, *21*, 1693–1696.
[11] R. Y. Ogura, S. Nakane, M. Morooka, M. Orihashi, Y. Suzuki, K. Noda, *Appl. Phys. Lett.* **2009**, *94*, 073308.
[12] L. Han, A. Islam, H. Chen, C. Malapaka, S. Zhang, X. Yang, M. Yanagida, B. Chiranjeevi, *Energy Environ. Sci.* **2012**, *5*, 6057–6060.
[13] J. Usagawa, S. S. Pandey, S. Hayase, M. Kono, Y. Yamaguchi, *Appl. Phys. Express* **2009**, *2*, 062203.
[14] Y. Noma, K. Lizuka, Y. Ogomi, S. S. Pandey, S. Hayase, *Jpn. J. Appl. Phys.* **2009**, *48*, 020213.
[15] C. Lan, H. Wu, T. Pan, C. Chang, W. Chao, C. Chen, C. Wang, C. Lin, E. Diau, *Energy Environ. Sci.* **2012**, *5*, 6460–6464.

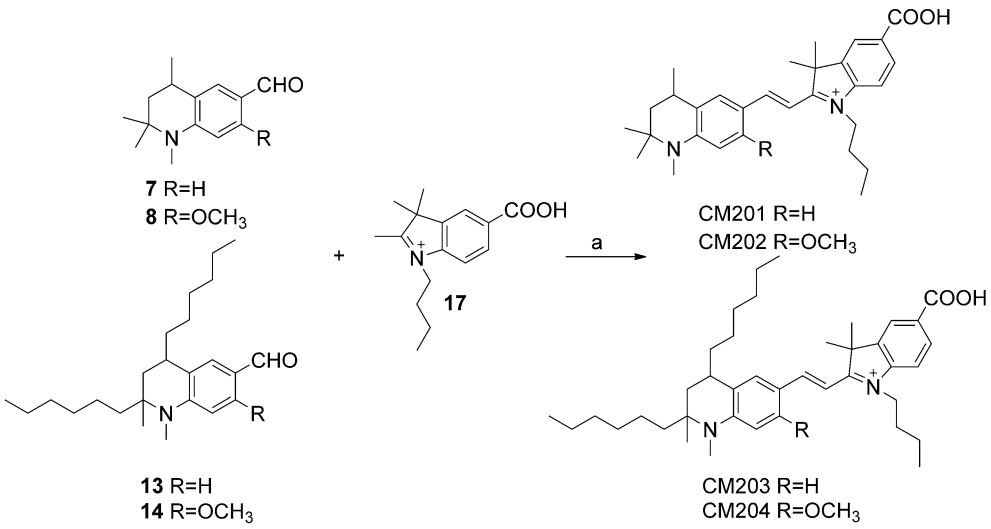

Scheme 3. Synthetic routes for the dyes CM201–CM204: a) piperidine, CH_3CN, 85 °C, 24 h.

[16] M. Kimura, H. Nomoto, N. Masaki, S. Mori, *Angew. Chem.* **2012**, *124*, 4447 – 4450; *Angew. Chem. Int. Ed.* **2012**, *51*, 4371 – 4374.
[17] J.-H. Yum, S.-R. Jang, P. Walter, T. Geiger, F. Nüesch, S. Kim, J. Ko, M. Grätzel, M. K. Nazeeruddin, *Chem. Commun.* **2007**, 4680 – 4682.
[18] J. Cong, X. Yang, Y. Hao, L. Kloo, L. Sun, *RSC Adv.* **2012**, *2*, 3625 – 3629.
[19] A. Hagfeldt, M. Grätzel, *Chem. Rev.* **1995**, *95*, 49 – 68.
[20] A. M. Bond, G. B. Deacon, J. Howitt, D. R. MacFarlane, L. Spiccia, G. Wolfbauer, *J. Electrochem. Soc.* **1999**, *146*, 648 – 656.
[21] K. Kalyanasundaram, M. Grätzel, *Coord. Chem. Rev.* **1998**, *177*, 347 – 414.
[22] J. E. Kroeze, N. Hirata, S. Koops, M. K. Nazeeruddin, M. Grätzel, J. R. Durrant, *J. Am. Chem. Soc.* **2006**, *128*, 16376 – 16383.
[23] F. Fabregat-Santiago, J. Bisquert, G. Garcia-Belmonte, G. Boschloo, A. Hagfeldt, *Sol. Energy Mater. Sol. Cells* **2005**, *87*, 117 – 131.
[24] M. Cheng, X. Yang, J. Li, C. Chen, J. Zhao, Y. Wang, Licheng Sun, *Chem. Eur. J.* **2012**, DOI:10.1002/chem.201200826.
[25] Y. Hao, X. Yang, M. Zhou, J. Cong, X. Wang, A. Hagfeldt, L. Sun, *ChemSusChem* **2011**, *4*, 1601 – 1605.
[26] C. Teng, X. Yang, C. Yang, S. Li, M. Cheng, A. Hagfeldt, L. Sun, *J. Phys. Chem. C* **2010**, *114*, 9101 – 9110.
[27] R. Chen, X. Yang, H. Tian, X. Wang, A. Hagfeldt, L. Sun, *Chem. Mater.* **2007**, *19*, 4007 – 4015.
[28] Y. Hao, X. Yang, J. Cong, H. Tian, A. Hagfeldt, L. Sun, *Chem. Commun.* **2009**, 4031 – 4033.
[29] J.-H. Yum, P. Walter, S. Huber, D. Rentsch, T. Geiger, F. Nüesch, F. D. Angelis, M. Grätzel, M. K. Nazeeruddin, *J. Am. Chem. Soc.* **2007**, *129*, 10320 – 10321.

Received: September 3, 2012
Published online on November 27, 2012